Proceedings of PRADS2016
4^{th}-8^{th} September, 2016
Copenhagen, Denmark

Using subdivision surfaces to address the limitations of B-spline surfaces in ship hull form modeling

Sebastian H. Greshake[1] and Robert Bronsart[1]

[1]University of Rostock, Germany

Abstract

The fundamental limitation of B-spline surfaces in hull form modeling is its restriction to quadrilateral surfaces. Aside of the necessity to compose hull forms of several patches, this results in an undesirable high number of control points and inefficient fairing. As a consequence, hull form modeling is a laborious task.

In contrast, subdivision is a method to define B-spline surfaces on control meshes of arbitrary topology. This allows to represent surfaces of any complexity with a single B-spline surface. Only a few control points are required and fairing is significantly simplified. In that, subdivision addresses exactly the fundamental limitation of B-spline surfaces in hull form modeling. This article briefly reviews the basics of a subdivision-based construction of B-spline surfaces, describes an algorithm to generate bicubic B-spline surfaces of any complexity, and shows its application in hull form modeling.

Keywords

Hull form; Subdivision surfaces; B-Splines

Introduction

Probably the most important information about a ship design is the hull form. To model a high-quality hull form is a major task of the ship design process. The quality of a hull form is measured in terms of fairness. This quality criterion requires curvature continuity as well as a minimal number of inflection points. Naturally, it is the designer's responsibility to minimize the number of inflection points. In contrast, curvature continuity is a property of the geometric representation of the hull form. Hence, the demand on quality that arises in the context of hull form modeling affects the geometric representation of the hull form.

In general, only a surface-based representation enables an unambiguous characterization of a hull form. Usually, tensor-product splines surfaces are employed for hull form representation. In most cases bicubic B-spline surfaces are used. Indeed, a cubic B-spline offers the best trade-off between a minimal degree and curvature continuity as required for a fair surface. Due to the topological limitation of tensor-product splines to quadrilateral surfaces, complex surfaces, such as typical hull forms, cannot be represented with a single tensor-product spline. However, hull surfaces are composed of several tensor-product spline patches, but this causes several implications on hull form modeling.

In general, discontinuities of different order are present between neighboring patches. At the first glance, this sounds rather mathematical. In fact, this implies a lack of definition of the hull form that is of technical importance. In this context, discontinuities of zeroth order between neighboring patches are the worst case. In practice, they cause the failure of analysis methods used for ship design and require substantial effort to handle. High-order discontinuities primarily affect the quality of a hull form representation in terms of fairness. Technically, the advantage of a good fairness of a hull surface is lower resistance and therefore lower fuel consumption of the ship. Due to discontinuous curvature or tangents the potential fairness of a hull form representation based on tensor-product splines is limited.

In order to keep discontinuities at least small, a large number of control points is required. Each patch requires a sufficient degree of freedom to be fitted in a continuous way to its neighbors. Hence, the manual definition of a hull surface is labor intensive, but even more sophisticated methods to construct hull forms, such as lofting curve networks, suffer from the limitation of tensor-product splines. As a consequence, hull form design is still a laborious task.

The limitation of tensor-product splines to quadrilateral surfaces causes the necessity to compose a hull form of several patches. To negotiate this limitation, attention has to be paid to its reason. The reason is that tensor-product splines are defined on regular control meshes. In order to address this limitation, a possibility to define spline surfaces on arbitrary topological control meshes is required. Naturally, this leads to the idea of subdivision surfaces. A certain class of subdivision surfaces generalizes tensor-product splines for control meshes of arbitrary topology. Certainly, the most important example is the algorithm of (Catmull and Clark, 1978), which generalizes bicubic B-spline surfaces.

Related work

Tensor-product B-splines are commonly used for hull form representation. However, the limitation of tensor-product splines to quadrilateral surfaces is recently identified by (Sharma et al., 2012) as incompatible to the generally non-quadrilateral surface of a hull form. Aside of the necessity to compose a hull form of several patches, this results in an undesirable high number of control points and inefficient fairing. To address the limitation of tensor-product splines is classified as a key issue to improve hull form modeling. This conclusion is justified by (Koelman and Veelo, 2013). In addition, a variety of possible solutions is provided. They can be roughly categorized into two groups: solutions that support the user in the construction of a set of ordinary tensor-product patches that join smoothly, and solutions that overcome the limitations of tensor-product splines in using an alternative surface construction. Though not identified as such, all proposed solutions of the second group belong to a certain class of subdivision surfaces.

This class of subdivision surfaces contains subdivision algorithms to generate B-spline surfaces on control meshes of arbitrary topology. From an analytical point of view they are spline surfaces with singularities at extraordinary points of the domain, but subdivision allows to remove those singularities. This is the appropriate setup to evaluate analytical properties of the surface exactly and therefore suitable to meet engineering demands. However, this setup requires the subdivision algorithm to be stationary. Refer to the subsequent section for a brief description of this approach to subdivision surfaces, or to the monograph of (Peters and Reif, 2008) for a comprehensive introduction in the uniform setting.

The most prominent examples are the subdivision algorithm of (Doo and Sabin, 1978), which generalizes biquadratic tensor-product splines, and the algorithm of (Catmull and Clark, 1978), which generalizes bicubic tensor-product splines. In addition, (Stam, 2001) and (Zorin and Schröder, 2001) provide generalizations for B-spline surfaces of arbitrary degree. All of these algorithms are stationary, but restricted to uniform B-splines.

Non-uniform B-splines are addressed by (Sederberg et al., 1998) for biquadratic and bicubic surfaces. However, the algorithms are non-stationary, but utilization of certain constraints for the knot vector yields a stationary algorithm, see (Sederberg et al., 2003). Furthermore, a special type of control point, the T-point, gives additional freedom to refine the control mesh locally. Another algorithm that generalizes non-uniform bicubic B-spline surfaces is described by (Müller et al., 2006) and later improved in (Müller et al., 2010). In vicinity of extraordinary points uniform subdivision is used, whereas non-uniform subdivision is restricted to regular parts of the control mesh. In fact, both algorithms blend between uniform and non-uniform subdivision. The first algorithm is non-stationary and the second algorithm is stationary. Finally, (Cashman et al., 2009) describes a stationary algorithm for non-uniform B-spline surfaces of any odd degree.

The most important application of non-uniform B-splines is the boundary behavior of open surfaces. A convenient boundary behavior of B-spline surfaces utilizes multiple knot lines on the domain boundaries. Furthermore, it is possible to define interior creases using multiple knot lines. However, none of the subdivision algorithms for non-uniform B-splines permits multiple knot lines at irregular knots. Hence, the application of non-uniform modeling features is limited to regular configurations.

Instead of using multiple knot lines, a local modification of the subdivision algorithm allows to introduce similar features to subdivision surfaces that are not constrained to certain topological configurations. A common modification for bicubic surfaces is given by (Hoppe et al., 1994) and later improved by (Biermann et al., 2000). An approach to integrate features in subdivision surfaces of arbitrary degree is described by (Stewart and Foisy, 2004).

Subdivision surfaces have gained wide popularity in other fields, such as animation movies. In this field they replaced tensor-product splines for the representation of complex objects. However, in the maritime industry they are still rarely used. An application of non-uniform subdivision surfaces for hull form design is shown by (Sederberg and Sederberg, 2010). Multiple knot lines are used to introduce features such as chines and knuckles to the hull form. The presented examples are rather simple and lack the complex transitions of the fore and aft body found in typical hull forms of merchant vessels. Due to the topological restriction of multiple knot lines to regular configurations, it would be interesting to see how such complexities are handled compared to the approach presented in this article. In (Greshake and Bronsart, 2015) it is shown that discontinuities between neighboring tensor-product patches limit the quality of a hull form representation. It is demonstrated that a hull form representation based on subdivision surfaces yields a significant improvement of quality due to the fact that those discontinuities are avoided. Finally, (Lee et al., 2004) proposes a method to generate a subdivision surface based on a network of ship lines. Indeed, they show that a subdivision-based representation of hull forms is compatible to this widely used method of hull form modeling. However, they use an ordinary Catmull-Clark subdivision surface and therefore they are not able to consider feature curves in the lines network.

Surface representation

Often tensor-product B-spline surfaces are simply called B-spline surfaces or, in order to refer to its most general form, they are called NURBS surfaces. The term *tensor-product* is usually omitted. However, in this context it is essential to refer explicitly to tensor-product or subdivision surfaces. Both terms may involve B-spline surfaces, but the difference that is emphasized is the mathematical approach to construct them. To clarify this difference, the subsequent material briefly reviews the fundamentals of tensor-product B-splines and then introduces the subdivision-based construction of B-spline surfaces. Providing this theoretical foundation to the community, the authors seek to resolve common misconceptions about subdivision surfaces and to legitimate them as suitable successor for tensor-product B-splines in the field of hull form modeling.

Tensor-product B-spline surfaces

A tensor-product B-spline surface is a continuous map

$$\mathbf{x} : \mathbf{\Sigma} \to \mathbb{R}^3 \tag{1}$$

where, for convenience, $\Sigma = [0,1]^2$ is restricted to the unit square, and

$$\mathbf{x}(s,t) = \sum_{i=0}^{n} \sum_{i=0}^{m} b_i^p(s) b_j^q(t) \mathbf{q}_{ij} \tag{2}$$

for all $(s,t) \in \Sigma$. The B-spline functions b_i^p and b_j^q are piecewise polynomials of degree p and degree q respectively, and $\mathbf{q}_{ij}$ forms a regular grid of control points. To compute the B-spline functions a bit more information is necessary: the knot vectors $[s_0, ..., s_{n+p+1}]$ and $[t_0, ..., t_{m+q+1}]$ respectively.

At the first glance, the mathematical setup might look excessive, but it is as simple as to take all pairs (s,t) from the unit square $[0,1]$ and to map them to points in $\mathbb{R}^3$ using equation 2. The particular properties of the B-spline functions ensure that the result will be a smooth surface.

Subdivision surfaces

The subsequent material introduces subdivision surfaces as generalized B-spline surfaces. It is a brief description of the essential concepts presented in the monograph of (Peters and Reif, 2008).

A generalized spline surface is a continuous map

$$\mathbf{x} : \mathbf{S} \to \mathbb{R}^3 \tag{3}$$

where $\mathbf{S}$ denotes the domain. The domain is composed of a set of indexed cells $\Sigma = [0,1]^2$ that are glued together. The domain is topologically unrestricted, what means that an arbitrary number of cells is allowed to meet in a common point.

The restriction of the generalized spline surface $\mathbf{x}$ to a certain cell of its domain

$$\mathbf{x}_i : \Sigma \ni (s,t) \mapsto \mathbf{x}(s,t,i) \in \mathbb{R}^3 \tag{4}$$

is called a patch. Indeed, this is identical to compose a complex surface of several patches. However, those patches are now treated rigorously as a single surface.

The next step is to utilize the notion of a generalized spline in order to define B-spline surfaces on control meshes of arbitrary topology. Initially, the restriction of the generalized spline surface to a certain patch is expressed in terms of equation 2. An example, which is reasonable in the context of hull form representation, is a bicubic tensor-product B-spline surface

$$\mathbf{x}_i(s,t) = \sum_{i=0}^{3} \sum_{i=0}^{3} b_i^3(s) b_j^3(t) \mathbf{q}_{ij} \tag{5}$$

where b_i^3 and b_j^3 shall denote uniform cubic B-spline functions and $\mathbf{q}_{ij}$ forms are regular grid of 4×4 control points. This example is shown in the left part of Figure 1. A simplified outline of the surface is shown in gray. The control mesh and the control points are shown in black.

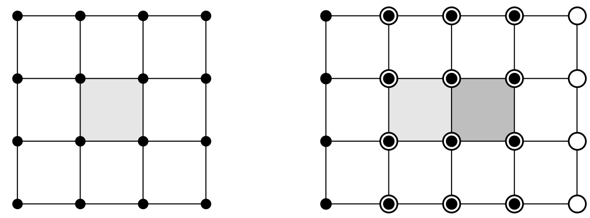

Figure 1. Connection of uniform bicubic B-spline patches with second-order continuity. Left: A simplified outline of a single patch and its control mesh. Right: Smooth connection of two patches. Curvature continuity is provided because both patches share a part of their control meshes.

To be useful, the generalized spline surface should offer the same smoothness properties as the patches. Therefore, neighboring patches are connected with second-order continuity as shown in the right part of Figure 1. Apparently, second-order continuity is obtained because both patches share a subset of their control points. However, to apply second-order continuity between neighboring patches it is much easier to define a single control mesh for all patches and to identify the corresponding subsets of the mesh with the individual patches. To clarify this concept, consider the example from Figure 1. The generalized bicubic B-spline surface consists of two patches and is defined on a single control mesh of 5×4 control points. The subset of 4×4 control points highlighted with black dots is identified with left patch, and the subset highlighted by empty circles is identified with the right patch. The overlap of both subsets ensures second-order continuity between both patches.

However, this does not enable irregular meshes as shown in Figure 2a. For simplicity only a part of the control mesh around the extraordinary control point in the center is shown. The rest of the mesh is assumed to be regular. Therefore, the outer ring of patches is well defined in terms of equation 5. In contrast, the inner patches do not posses any tensor-product representation due to the irregularity of the control mesh. For the patches incident to extraordinary point it is not clear what points should be chosen to define a regular subset of 4×4 control points. Refer to the highlighted patch and control points in Figure 2a for confirmation.

At this stage, a surface representation is introduced that allows to define a B-spline surface composed of sev-

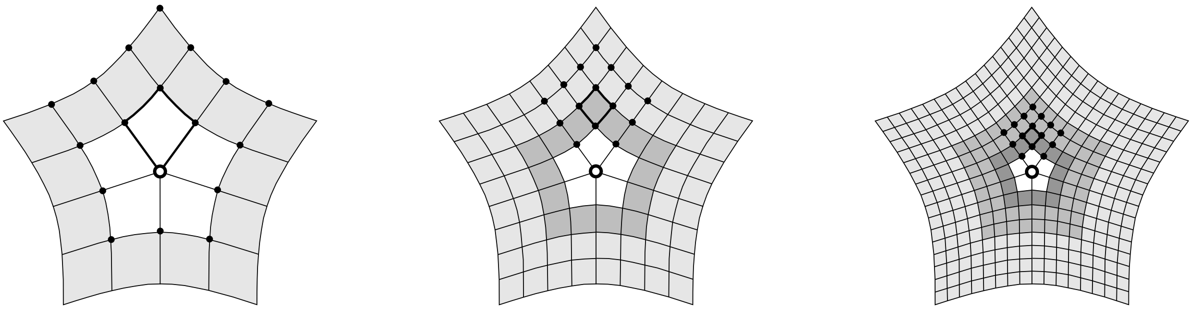

(a) Initial configuration. (b) First subdivision. (c) Second subdivision.

Figure 2. A generalized spline surface with an irregular control mesh. Patches incident to the extraordinary control point cannot be defined in terms of tensor-product splines. However, subdivision allows to add further rings of tensor-product spline patches in vicinity of the extraordinary point.

eral tensor-product B-spline patches on a single control mesh. Furthermore, a certain level of continuity between neighboring patches is guaranteed. This representation is called a generalized B-spline surface, but the ultimate goal to define B-spline surfaces on irregular control meshes is, so far, not achieved. The final step to enable irregular control meshes requires an instrument called *subdivision*.

One step of subdivision splits every patch of the surface into four patches. The surface does not change, but the number of patches used to represent the surface increases. The challenge is to find a new control mesh for the patches that satisfies this condition. For the regular case, classical spline theory provides the appropriate tools for this task: knot refinement. The contribution of (Catmull and Clark, 1978), (Doo and Sabin, 1978), and other authors mentioned above is to provide a generalization of knot refinement for extraordinary configurations of the control mesh. This is called a subdivision algorithm.

To refine the control mesh allows to add another ring of tensor-product B-spline patches in vicinity of the extraordinary point as shown in Figure 2b. It is easily verified that the new patches are connected with second-order continuity to its neighbors. A further step of subdivision adds a further ring of tensor-product splines, see Figure 2c. Thus, subdivision generates a growing tensor-product representation of a generalized spline surface in vicinity of extraordinary points. Indeed, this is the appropriate setup to access analytical properties of a generalized spline exactly, even in the presence of extraordinary points.

The generalized spline surface inherits its continuity properties form the regular connection of neighboring patches, except at extraordinary points. To analyze continuity at the extraordinary point is thoroughly dealt with in the monograph of (Peters and Reif, 2008). In fact, the major task to construct a subdivision surface is to define subdivision rules for extraordinary points that guarantee a sufficient level of continuity.

Generalized bicubic B-spline surface

In this article, the subdivision algorithm of (Catmull and Clark, 1978) is used. The algorithm is a generalization of knot insertion for uniform cubic tensor-product B-splines. In addition, the surface may contain creases and corners as features. This is realized with a subset of the extensions proposed by (Biermann et al., 2000). In general, the surface is curvature continuous (G^2) everywhere, but at extraordinary points it is only normal continuous (G^1).

Feature definition

Features of the surface are defined based on tags applied to the control mesh. However, the choice of tags may be interdependent.
Edge tags: Edges of the control mesh can be tagged to be smooth or crease. By default, edges are smooth, except for boundary edges that are always creases.
Vertex tags: By default, vertices are smooth. Vertices incident to exactly two crease edges must be either tagged as a crease vertex or as a corner vertex. Vertices incident to a single crease edge are tagged as a dart vertex. Vertices incident to three or more crease edges are always tagged as corner vertices.

Control points

Every subdivision step results in a new control mesh. The rules to compute new control points are given in this section. The presentation of the rules is based on the article of (Biermann et al., 2000), but all rules are generalized for non-quad meshes. However, this generalization reproduces the original rules in case of a quad mesh.
Face points: For each face of the control mesh a new control point

$$\mathbf{f}_i = \frac{1}{n} \sum_{i=1}^{n} \mathbf{p}_i \tag{6}$$

is computed as the average of the n vertices $\mathbf{p}_i$ defining the face.

Edge points: For each smooth edge of the control mesh a new control point

$$\mathbf{e}_i = w_1\mathbf{p}_1 + w_2\mathbf{p}_2 + \frac{1}{4}(\mathbf{f}_1 + \mathbf{f}_2) \quad (7)$$

is computed as the weighted average of the vertices $\mathbf{p}_1$ and $\mathbf{p}_2$ defining the edge and the face points $\mathbf{f}_1$ and $\mathbf{f}_2$ of the two faces incident to the edge. The choice of weights w_1 and w_2 depends on the tags of $\mathbf{p}_1$ and $\mathbf{p}_2$. If both vertices are (not) smooth the weights are simply $w_1 = w_2 = 1/4$. If one vertex is smooth and the other vertex is not smooth, the weights are parametrized by θ_k where k is the number of faces in the sector of the edge. The notion of a sector is illustrated in Figure 3.

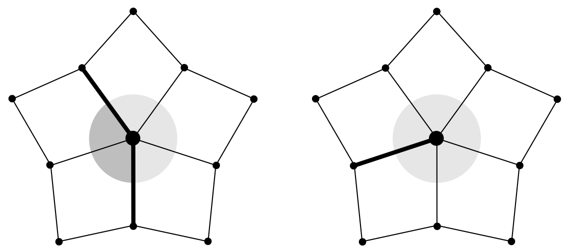

Figure 3. Crease edges of the control mesh are shown in bold and divide the mesh around the central vertex into sectors. Left: The mesh is divided into a sector of two faces and a sector of three faces. Right: A single sector of five faces, which is introduced by a crease that terminates in a dart.

Given the definition of a sector, the weight of the non-smooth vertex is $w = \frac{1}{2}\cos^2(\theta_k)$ and the weight of the smooth vertex is $w = \frac{1}{2}\sin^2(\theta_k)$ with $\theta_k = \pi/(4k)$ for a corner vertex, $\theta_k = \pi/(2k)$ for a crease vertex and $\theta_k = \pi/k$ for a dart vertex. The definition of θ_k for corner vertices is modified in comparison to the original rules of (Biermann et al., 2000).

For each crease edge of the control mesh a new control point

$$\mathbf{e}_i = \frac{1}{2}\mathbf{p}_1 + \frac{1}{2}\mathbf{p}_2 \quad (8)$$

is computed as the average of the vertices $\mathbf{p}_1$ and $\mathbf{p}_2$ defining the edge.

Vertex points: The rule for a new vertex point depends on the tag of the vertex. For each smooth or dart vertex of the control mesh a new control point is defined by

$$\mathbf{v}_i = \frac{1}{n^2}\sum_{i=1}^{n}\mathbf{f}_i + \frac{1}{n^2}\sum_{i=1}^{n}(\mathbf{p}_c + \mathbf{p}_i) + \frac{n-3}{n}\mathbf{p}_c \quad (9)$$

with $\mathbf{f}_i$ are the face points of the faces incident to the vertex, $\mathbf{p}_i$ are the surrounding vertices and $\mathbf{p}_c$ is the position of the old vertex. For each crease vertex a new control point

$$\mathbf{v}_i = \frac{1}{8}\mathbf{p}_1 + \frac{3}{4}\mathbf{p}_c + \frac{1}{8}\mathbf{p}_2 \quad (10)$$

is computed as the weighted average of the adjacent crease vertices $\mathbf{p}_1$, $\mathbf{p}_2$ and the position of the old vertex $\mathbf{p}_c$. For each corner vertex a new control point is simply given by $\mathbf{v}_i = \mathbf{p}_c$.

Hull form modeling

The first step to model a hull form is to define a set of feature curves that gives a rough outline of the surface and its breakdown into regions. The second step is to define a surface, or a sufficiently dense set of curves, that meets the constraints imposed by the feature curves and geometrically describes the regions in between.

Feature curves

Feature curves subdivide the hull form into several regions and define the geometric transition of neighboring regions. Three basic types of features curves are used for hull form modeling: knuckle curves, tangent curves, and smooth curves.

Knuckle curves: A hull surface is position continuous (G^0) across a knuckle curve. Neither the normals nor the curvature agree on the knuckle. A variant of a knuckle is an angle curve with a prescribed angle between the normals.

A knuckle curve is introduced to the generalized bicubic B-spline surface with a chain of crease edges. Dart vertices may be used in order to fade out knuckles smoothly.

Creases provide an intuitive way to define knuckles. However, the subdivision rules for creases that are presented above are equivalent to the natural boundary condition. As a consequence, the Gaussian curvature is always zero on a knuckle. This is potentially unfavorable in hull form modeling and affects the implementation of tangent curves. Several knuckle curves may meet at a corner, but the angle between two consecutive knuckles is limited to $\alpha \leq 180°$.

Tangent curves: A hull surface is normal continuous (G^1) across a tangent curve. Normal continuity requires the normals to agree, but normal direction may change along the tangent curve. In general, the curvature disagrees.

Tangent curves are realized on the generalized B-spline surface similar to knuckles. A chain of crease edges identifies the tangent curve. In addition, all faces incident to the crease edges are restricted to a common plane. This guarantees a common normal vector on the crease. However, this construction is also curvature continuous because the curvature component across a crease coincides and is always zero.

In comparison to the general definition of a tangent curve this implementation is quite limited. The surface is always G^2 across a tangent curve as opposed to the general definition that requires only G^1 continuity. Furthermore, it is not possible to change the normal direction along the tangent curve. Nevertheless, this construction is useful to realize two major applications of tangent curves in hull form modeling: the flat of side and the flat of bottom.

Smooth curves: A hull form is curvature continuous (G^2) across a smooth curve. A smooth curve on the generalized B-spline surface is simply identified by a chain of smooth edges.

Modeling a Ro-Ro vessel

Figure 4 shows the hull form of a modern Ro-Ro vessel. A single generalized B-spline surface is used to represent the entire hull form. A lines plan, which is inferred from the surface, is shown in Figure 6. It provides the details about the hull form features that are realizable based on generalized bicubic B-spline surfaces. Furthermore, the lines plan conveys an impression of the fairness that is provided by generalized B-spline surfaces. It is emphasized that fair lines are supplied by default.

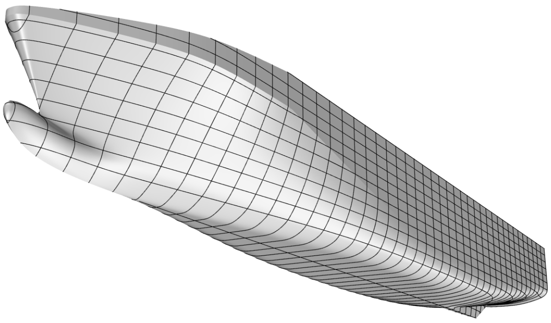

Figure 4. Hull form of a modern Ro-Ro vessel that is entirely represented by a single generalized B-spline surface. The vessel has a bulbous bow, a flat side and bottom, a pram type stern, and a skeg. The transition of the flat side into the bilge initially takes the form of a knuckle that gradually disappears towards the middle body.

Conventional hull form modeling, that is lines drawing but also most lines-based modeling software, is based on the methodology of interpolation. This method may come in two fashions: either additional lines are generated from the interpolation of an existing lines, alternatively surface patches that interpolate the lines are generated. Whatever flavor is employed, it is well-known that interpolation tends to oscillation. This tendency makes fairing of lines time-consuming. In addition, oscillations are the reason that it is almost impossible to change a given set of lines later on. Even small changes may result in heavy oscillations of other lines, making any previous efforts on fairing worthless. In contrast, a B-spline surface is based on the methodology of approximation. The control mesh of a B-spline surface is a coarse outline of the desired shape. The final surface approximates the control mesh with well-defined behavior. Most importantly, the surface does not oscillate more often than its control mesh oscillates, also known as the variation diminishing property.

Unfortunately, this advantage of B-spline surfaces cannot be utilized with tensor-product surfaces. The representation of hull forms needs several patches that are continuously fitted to each other, but this requires a high number of control points. Most control points are required to maintain smooth transitions between neighboring patches. However, it is difficult to minimize oscillations when the number of control points is high and a lot of points are constrained by continuity requirements. This problem is avoided with generalized B-spline surfaces. The representation of hull forms requires only a small number of control points as shown in Figure 5. The control mesh consists of about 120 control points, where approximately 15 control points are used in longitudinal direction and less than ten points are used in transverse direction. The small number of control points in any direction simplifies the minimization of oscillations significantly.

The lines plan shown in Figure 6 shows various hull form features such as a bulbous bow, an advanced transition of the flat side to the bilge, or a pram-type stern. These design decisions in terms of hull features are represented in terms of the control mesh, shown in Figure 5.

Forebody: A bulbous bow is fitted to the hull form. Essentially, twelve control points are used to define the shape and area of the bulbous bow. Four of them are placed in front of the forward perpendicular. The boundary points define the profile of the bulbous bow and the interior points are used, in conjunction with the lower four control points at the forward perpendicular, to control the volume. The boundary points are placed on the center plane, the lower interior control points are placed near to center plane, and the upper interior control points are placed further out. This gives the sections of the bulbous bow the desired wedge shape. The axis of the bulbous bow features a slope downwards as required for a gooseneck type. The slope corresponds to the downward slope of the longitudinal control mesh edges. The lower four control points of the first station behind the forward perpendicular are used to control the transition of the bulb-shaped sections to V-shaped sections.

Around the forward perpendicular bulb-shaped sections are realized. Afterwards, V-shaped sections are intended that gradually change to U-shaped sections towards the middle body. Accordingly, the control points are placed on an imaginary V that changes gradually to an U. The rate at which the control point arrangement changes determines how fast the sections change from V-type to U-type.

To minimize the overall curvature of the forebody, the pronounced V-shaped sections at the bow are joined with the vertical top of the hull form in a knuckle. The knuckle terminates in a corner and is connected to the flat of side, which initially takes the form of a knuckle too. However, hydrodynamics demand a smooth transition of the flat side into the bilge below the waterline, but, as usual in hull form design, G^1 continuity is sufficient. The knuckle and the flat of side are both identified by a chain of crease edges. They are highlighted as bold edges in Figure 5. The faces above the crease edges are all vertical, but the the incident faces below the creases are not vertical everywhere. Initially, the faces are placed according to the V-shape of the sections. As the section-type changes from V to U, the flare vanishes. At the middle body they are also vertical what ensures a common tangent of bilge and flat side. The flat of bottom is realized similar to the flat of side. However, the transition of the flat bottom to the rest of the hull form is smooth everywhere and the incident faces are all horizontal.

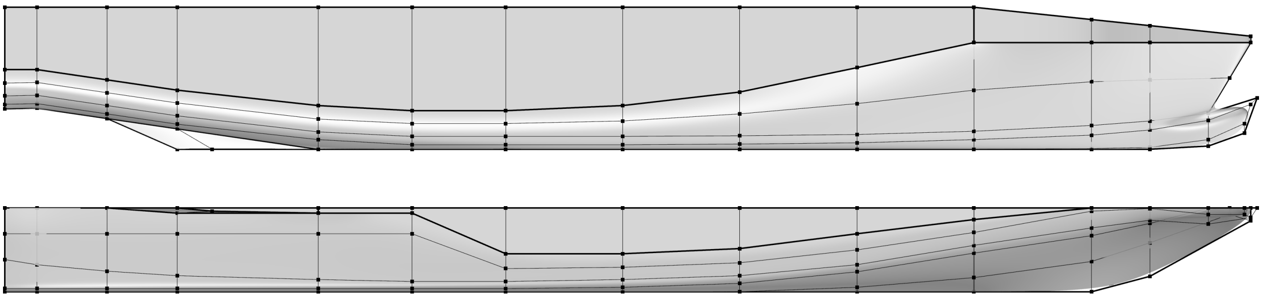

Figure 5. Control mesh of the generalized B-spline surface that is used for the representation of a modern Ro-Ro vessel. The mesh consists of about 120 control points, where approximately 15 control points are used in longitudinal direction and less than ten points in transverse direction. Bold lines denote crease edges and thin lines denote smooth edges.

Afterbody: A pram type stern with a trim wedge is realized. Viewed laterally, the longitudinal edges of the control mesh are placed on a line with an angle towards the baseline that is the same as the desired angle between the buttocks and the baseline. An angle of about 10° is chosen. Towards the middle body this angle is gradually reduced until the longitudinal edges are horizontal. The length of this transition zone controls the radius in the buttocks. At the transom the longitudinal edges point downwards in order to introduce a trim wedge to the hull form. The submergence of the trim wedge is $t = 30\,\text{cm}$ at the design draft.

A skeg is introduced to the hull form in order to assist course stability of the vessel. Crease edges are employed to model the boundaries of the skeg as knuckles. For a smooth transition of the skeg into the flat bottom a horizontal face is placed between the forward end of the skeg and the rear point at which the flat bottom starts to expand transversally.

Conclusions

Subdivision is a method to define B-spline surfaces on control meshes of arbitrary topology. In that, subdivision addresses the fundamental limitation of B-splines in hull form modeling: its limitation to quadrilateral surfaces. To give credit to this contribution, this article refers to subdivision surfaces as generalized B-spline surfaces.

Relieved from the limitation to four-sided surfaces, complex hull forms can be entirely represented by a single B-spline surface. This simplifies hull form modeling significantly, but potentially eases downstream usage of the hull geometry as well because error-prone inconsistencies of the hull form geometry are avoided. The simplification of hull modeling is particularly evident when it comes to fairing. This term requires curvature continuity as well as a minimal number of inflection points, where the latter is the critical point in conventional lines-based modeling. In contrast, a B-spline surface does not oscillate more often than its control mesh does and hence gives the hull designer precise control in this manner.

It is described, how various hull form features are represented in terms of the control mesh. The lines plan in Figure 6 gives the details about these features, but likewise the given main dimensions and coefficients illustrate the precise control about the hull characteristics.

Generalized B-spline surfaces are proposed to replace tensor-product B-splines for hull form representation. The bicubic B-spline surface described in this article offers a reasonable trade-off between a low degree, curvature continuity, and additional modeling features. They are successfully utilized for the representation of knuckles and, with limitations, tangent curves on the surface. However, the curvature across tangent curves and knuckles is always zero. This is potentially unfavorable in the context of hull modeling and future work will focus on this limitation.

References

Biermann, H., Levin, A., and Zorin, D. (2000). Piecewise smooth subdivision surfaces with normal control. In *Proceedings of the 27th Annual Conference on Computer Graphics and Interactive Techniques*, SIGGRAPH '00, pages 113–120. ACM Press/Addison-Wesley Publishing Co.

Cashman, T. J., Augsdrfer, U. H., Dodgson, N. A., and Sabin, M. A. (2009). NURBS with extraordinary points: High-degree, non-uniform, rational subdivision schemes. *ACM Trans. Graph.*, 28(3):46:1–46:9.

Catmull, E. and Clark, J. (1978). Recursively generated b-spline surfaces on arbitrary topological meshes. *Computer-Aided Design*, 10(6):350–355.

Doo, D. and Sabin, M. (1978). Behaviour of recursive division surfaces near extraordinary points. *Computer-Aided Design*, 10(6):356–360.

Greshake, S. H. and Bronsart, R. (2015). High quality ship hull form representation based on subdivision surfaces. In *International Conference on Computer Applications in Shipbuilding 2015*, volume 2, pages 81–90.

Hoppe, H., DeRose, T., Duchamp, T., Halstead, M., Jin, H., McDonald, J., Schweitzer, J., and Stuetzle, W. (1994). Piecewise smooth surface reconstruction. In *Proceedings of the 21st Annual Conference on*

Computer Graphics and Interactive Techniques*, SIGGRAPH '94, pages 295–302. ACM.

Koelman, H. J. and Veelo, B. N. (2013). A technical note on the geometric representation of a ship hull form. *Computer-Aided Design*, 45(11):1378 – 1381.

Lee, K.-Y., Cho, D.-Y., and Kim, T.-W. (2004). Interpolation of the irregular curve network of ship hull form using subdivision surfaces. *Computer-Aided Design and Applications*, 1(1):17–23.

Müller, K., Fünfzig, C., Reusche, L., Hansford, D., Farin, G., and Hagen, H. (2010). Dinus: Double insertion, nonuniform, stationary subdivision surfaces. *ACM Trans. Graph.*, 29(3):25:1–25:21.

Müller, K., Reusche, L., and Fellner, D. (2006). Extended subdivision surfaces: Building a bridge between NURBS and catmull-clark surfaces. *ACM Trans. Graph.*, 25(2):268–292.

Peters, J. and Reif, U. (2008). *Subdivision surfaces*. Springer.

Sederberg, M. T. and Sederberg, T. W. (2010). T-splines: a technology for marine design with minimal control points. In *2nd Chesapeake Power Boat Symposium 2010*, pages 250–255.

Sederberg, T. W., Zheng, J., Bakenov, A., and Nasri, A. (2003). T-splines and t-NURCCs. *ACM Trans. Graph.*, 22(3):477–484.

Sederberg, T. W., Zheng, J., Sewell, D., and Sabin, M. (1998). Non-uniform recursive subdivision surfaces. In *Proceedings of the 25th Annual Conference on Computer Graphics and Interactive Techniques*, SIGGRAPH '98, pages 387–394. ACM.

Sharma, R., Kim, T.-w., Storch, R. L., Hopman, H. J., and Erikstad, S. O. (2012). Challenges in computer applications for ship and floating structure design and analysis. *Computer-Aided Design*, 44(3):166–185.

Stam, J. (2001). On subdivision schemes generalizing uniform b-spline surfaces of arbitrary degree. *Computer Aided Geometric Design*, 18(5):383–396.

Stewart, I. F. and Foisy, A. R. (2004). Arbitrary-degree subdivision with creases and attributes. *Journal of Graphics Tools*, 9(4):3–17.

Zorin, D. and Schröder, P. (2001). A unified framework for primal/dual quadrilateral subdivision schemes. *Computer Aided Geometric Design*, 18(5):429 – 454.

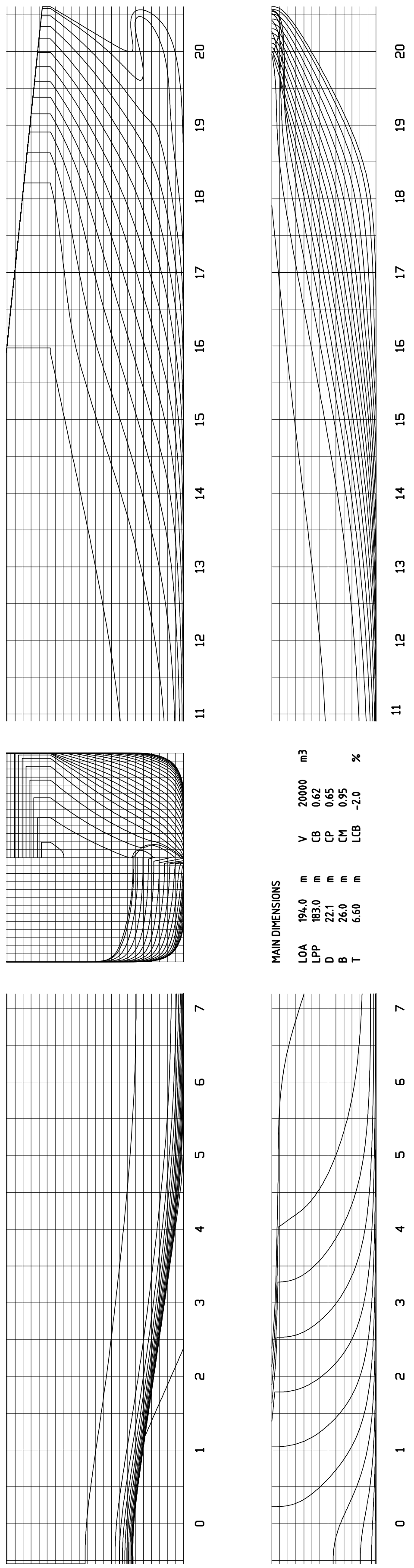

Figure 6. Lines plan of the Ro-Ro vessel shown in Figure 4.